Absolute differential and total cross sections for single electron capture in low-energy Kr^+-Ar collisions

H. Martínez and P. G. Reyes
Instituto de Física, Universidad Nacional Autónoma de México, Apartado Postal 48-3, 62251 Cuernavaca, Morelos, Mexico
(Received 13 July 1998; revised manuscript received 4 September 1998)

Absolute differential and total cross sections for single electron capture were determined from Kr^+ ions on Ar in the energy range 0.3–5.0 keV. Using reduced variables [$\tau = E\theta$ vs $\theta \sin(\theta) d\sigma/d\Omega = \rho$], we deduced, from the experimental differential cross sections, that the electron capture channel ''opens'' at a critical projectile-target separation between $1.63a_0$ and $2.21a_0$ in the present energy range and that at least two different processes are involved. The total cross section for single electron capture is compared with other available measurements. These results give a general shape of the curve for single electron capture cross sections for the Kr^+-Ar system in a wide range of energy. [S1050-2947(99)00203-6]

PACS number(s): 34.70.+e

I. INTRODUCTION

Charge-changing atomic collision processes in keV energies are of considerable importance to environments ranging from tokamak plasmas to planetary atmospheres. In previous papers [1,2] we reported cross-section measurements on the Kr^+-He and Kr^+-Xe systems. To complement these studies and to provide more information on single electron capture in $Kr^+ +$ (rare gas) reactions, we report absolute measurements of the differential and total cross sections of single electron capture for Kr^+ collisions with Ar atoms. The energy range of the present study is 0.3–5.0 keV and the laboratory scattering angle is between $-2°$ and 2°. In particular, the reasons for choosing the Kr^+-Ar systems for study were the following. (i) A work on total cross sections at low energy exhibiting several structures was published previously [3] and we felt that the measurements of differential cross sections serve as a more sensitive proof for the collision dynamics regarding the potential-energy curves and interference phenomena. (ii) To the best of our knowledge, there are no absolute cross sections reported in the keV-energy range.

II. EXPERIMENT

The experimental apparatus and technique needed to generate the fast ion beam are essentially the same as that reported recently [4]. Briefly, the Kr^+ ions formed in an arc discharge source, accelerated to the desired energy, were focused and velocity analyzed by a Wien filter, and passed through a series of collimators before entering the gas target cell, consisting of a cylinder 2.5 cm in length and diameter, with a 2-mm-wide, 6-mm-long exit aperture. All other apertures and slits had knife edges. The target cell was located at the center of a rotatable, computer-controlled vacuum chamber that moved the whole detector assembly, which was located 47 cm away from the target cell. A precision stepping motor ensured a high repeatability in the positioning of the chamber over a large series of measurements. The detector assembly consisted of a Harrower-type parallel-plate analyzer and two channel-electron multipliers (CEMs) attached to its exit ends. The neutral beam (Kr^0) passed straight through the analyzer and impinged on a CEM so that the neutral counting rate could be measured. Separation of charged particles occurred inside the analyzer, which was set to detect the Kr^+ ions with the lateral CEM. The CEMs were calibrated *in situ* with low-intensity Kr^0 and Kr^+ beams, which were measured as a current in a Faraday cup by a sensitive electrometer. The uncertainty in the detector calibration was estimated to be less than 3%. A retractable Faraday cup was located 33 cm away from the target cell, allowing the measurement of the incoming Kr^+ ion-beam current.

Under the thin target conditions used in this experiment, the differential cross sections for the Kr^0 formation were evaluated from the measured quantities by the expression

$$\frac{d\sigma(\theta)}{d\Omega} = \frac{I_f(\theta)}{I_0 n l}, \tag{1}$$

where I_0 is the number of Kr^+ ions incident per second on the target (typically $\sim 2.2\times 10^8$ particles/s), n is the number of Kr atoms per unit volume (typically 1.2×10^{13} atoms/cm^3); l is the length of the scattering chamber ($l = 2.5$ cm), and $I_f(\theta)$ is the number of Kr^0 particles per unit solid angle per second detected at a laboratory angle θ with respect to the incident beam direction (typically $\sim 6.6\times 10^{10}$ particles/s). The total cross section σ for the production of the Kr^0 particles was obtained by the integration of $d\sigma/d\Omega$ over all angles, that is

$$\sigma = 2\pi \int_0^{\pi} \frac{d\sigma}{d\Omega} \sin(\theta) d\theta. \tag{2}$$

Extreme care was taken when the absolute differential cross section was measured. The reported value of the angular distribution was obtained by measuring it with and without gas

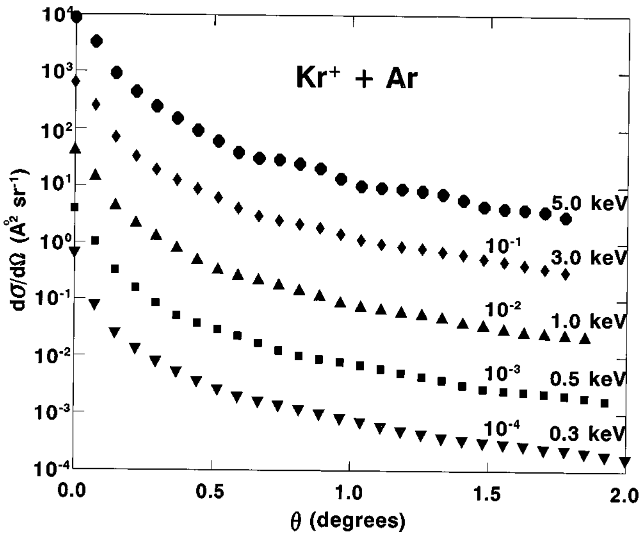

FIG. 1. Measured absolute differential cross sections for single electron capture.

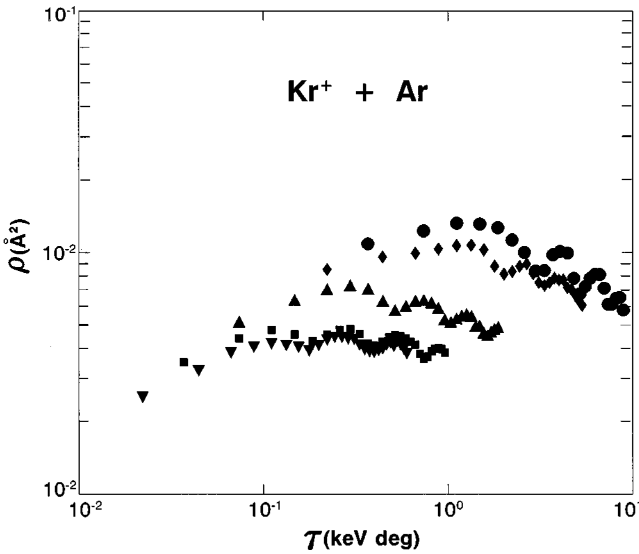

FIG. 2. Experimental reduced differential cross sections for single electron capture of Kr^+ ions in Ar: ●, 5.0 keV; ◆, 3.0 keV; ▲, 1.0 keV; ■, 0.5 keV; ▼, 0.3 keV.

in the target cell with the same steady beam. Then point-to-point substraction of both angular distributions was carried out to eliminate the counting rate due to neutralization of the Kr^+ beam on the slits and those arising from background distributions. The Kr^+ beam intensity was measured before and after each scan. Measurements not agreeing to within 5% were discarded. Angular distributions were measured on both sides of the forward direction to ensure they were symmetric. The estimated rms error was 15%, while the total cross sections were reproducible to within 10% from day to day.

Several runs were made at different gas target pressures and $d\sigma/d\Omega$ was determined for each run. These were compared in order to estimate the reproducibility of the experimental results as well as to determine the limits of the ''single-collision regime'' since the differential and total cross sections reported are absolute.

In the present work changes were not observed in the absolute values with respect to the ion source conditions. Also, no variation in the distributions was detected over a target pressure range of 0.2–0.6 mTorr.

Several sources of systematic errors are present and have been discussed in a previous paper [4]. The absolute error of the reported cross sections is believed to be less than $\pm 15\%$. This estimate represents both random and systematic errors.

III. RESULTS AND DISCUSSION

Measurements of differential cross sections have been performed at laboratory angles of $-2° \leqslant \theta \leqslant 2°$ and collision energies of $0.3 \leqslant E_{\mathrm{lab}} \leqslant 5.0\,\mathrm{keV}$. Differential cross sections for single electron capture of Kr^+ in Ar are presented in Fig. 1 for laboratory energies of 0.3, 0.5, 1.0, 3.0, and 5.0 keV. All curves plotted in Fig. 1 show a monotonic decrease in the differential cross section with increasing angle. The electron capture data show slight structures in the differential cross sections, which tend to disappear as the incident energy decreases. This is presumably due either to curve crossing of the potential-energy surfaces for the initial and final states or to Demkov-type oscillations in the electron capture probability as a function of the scattering angle. A method that has been used extensively in the past to analyze collision cross sections is that in which the angular distribution is expressed in reduced variables [$\tau = E\theta$ vs $\rho = \theta \sin(\theta) d\theta/d\Omega$] as described by Smith, Marchi, and Dedrick [5]. In this normalized form, all electron capture data for a charged particle and a given velocity-independent interaction potential would fall on a general curve that is determined only by this interaction potential and each τ value then belongs to a certain value of the collisional impact parameter b. Thus data taken at different energies and plotted in (τ,ρ) coordinates should fall on a single curve. However, as this approach is based on an approximation to a series expansion, in some points, as τ increases, the approximation will no longer be valid and data at different energies will inevitably diverge. Figure 2 shows the angular distributions of the data on Fig. 1 as a function of the reduced variables; the shape of the curves is identical for all the energies. This is in agreement with the ''scaling principle'' and allows us to have a common curve $\rho(\tau)$. Three features of the reduced cross section curves are worth noting. First, the curves at low energy show a tendency to fall into a single pattern in accordance with the expectations arising from the scaling law [5], with a maximum independent of energy at $\tau \approx 0.11\,\mathrm{keV\,deg}$. Second, for the 1.0-keV data, a small systematic horizontal shift is observed between the low-energy curves and the high-energy curves. At this energy a structure is observed at $\tau \approx 0.3\,\mathrm{keV\,deg}$. Third, for energies above 3.0 keV, the high-energy data clearly fall closer to another single curve with a slight horizontal shift as the energy increases. There is a characteristic structure that occurs at a constant value of $\tau \approx 1.4\,\mathrm{keV\,deg}$ for 3.0 keV and $\tau \approx 1.5\,\mathrm{keV\,deg}$ for 5.0 keV. The features that occur at the same value of τ for different energies indicate that they originate at a common region of the interaction potential since constant τ implies nearly constant impact parameter and the

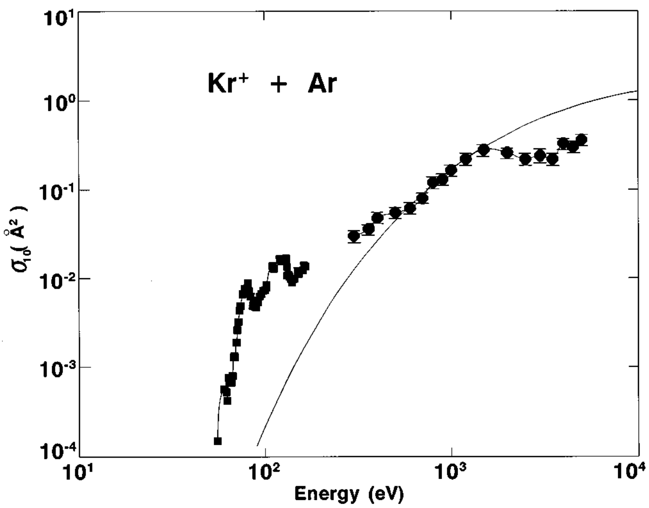

FIG. 3. Total cross sections for single electron capture of Kr^+ ions in Ar: ●, present measurements; ■, from Ref. [8]; ——, semiempirical calculation of Olson [9].

distance of closest approach [5]. In this particular case, the impact parameters b were evaluated using an exponentially Coulomb potential [5]. In the present case the experimental results show three features, one of which is around $\tau \approx 0.11$ keV deg (corresponding to the parameter $b \approx 2.21a_0$) at low energies, the second one at $\tau \approx 0.3$ keV deg ($b \approx 1.98a_0$) at 1.0 keV, and the third one around $\tau \approx 0.45$ keV deg ($b \approx 1.63a_0$) at high energies. The impact parameter estimated through the exponentially shielded Coulomb potential is probably not accurate, but it is sufficient for the present purpose. These results suggest that when the Kr^+ projectile penetrates into a critical projectile-target separation (here corresponding to b between $1.63a_0$ and $2.21a_0$) the electron capture channel ''opens.'' It is not possible at this time to identify the specific channels.

The differential cross sections have been integrated to yield total cross sections. A comparison of a previous measurement [3] on single-electron-capture cross sections and ours is shown in Fig. 3. Although there is no overlap of the two sets of data, the shape of the cross-section curve of Ref. [3] and present measurements indicate that the data for both measurements are mutually consistent. These results give a general shape of the whole curve of single-electron-capture cross sections for the Kr^+-Ar system in a wide range of energy.

Figure 3 shows several interesting structures in the cross section. Previous investigations also reveal structures at low energies in the $Ne^+ + Ar$ reaction [3]. It is also intriguing that the structure at low energies in the cross sections of the $Kr^+ + Ar$ system is much more prominent than for the $Ne^+ + Ar$ case. Notice that the threshold energy for $Kr^+ + Ar \rightarrow Ar^+ + Kr$ ($|\Delta E| = 1.76$ eV) is large enough for $Kr^+ + Ar \rightarrow Kr^+ + Ar^+ + e$ ($|\Delta E| = 15.759$ eV) to proceed; perhaps this circumstance is somehow connected with the structure in the cross section. Although it is not possible to identify the specific processes from the present studies, the general shapes of the curves in Figs. 2 and 3 suggest that at least two different processes are involved.

Until now, there has been no theoretical study (to our knowledge) dealing with the above process to compare with our experimental results in this energy range. Since potential-energy curves are not generally available for the inhomogeneous rare-gas diatomic ions, it is impractical to attempt a detailed theoretical exposition. In any event, it is not entirely clear how to calculate the transition probabilities between two sets of interacting curves [6] even for simpler systems [7,8]. It thus appears desirable that a detailed theoretical analysis be carried out to further check this behavior. It is nevertheless possible to explain some of these observations in terms of ''curve crossing'' without having accurate potential curves. Let us consider the behavior of some of the cross sections in the intermediate-energy range, as is next illustrated, using the semiempirical model of Olson [9]. The total single-electron-capture cross sections are calculated with the universal reduced cross section of Olson [9] using $R_c = 1.98a_0$ (which was taken from the experimental reduced differential cross section at 1.0 keV) and the coupling matrix element $H_{12} = 0.198$ a.u. [which was calculated through the expression $H_{12} = R^* \exp(-0.86R^*)$, where $R^* = \frac{1}{2}(\alpha + \gamma)R_c$]. We used $\frac{1}{2}\alpha^2 = 15.759$ eV as the effective ionization potential of the target and $\frac{1}{2}\gamma^2 = 13.999$ eV as the Kr^+ ground-state electron affinity; $|\Delta V'(R_c)|$ was fitted until the experimental cross section at 1.0 keV was obtained, giving thus a value of 3.8 a.u./a_0. The results of this calculation are shown in Fig. 3 (solid line). Although the Olson model calculation is not expected to be highly reliable, the calculation of σ_{10} is seen to agree in shape with the present measurements over the energy range 0.5–1.5 keV. At low energies, the experimental data of Maier [3] lie above the Olson model calculations, with deviations of ~100%.

IV. SUMMARY

Differential and total cross sections for single electron capture in Kr^+-Ar collisions were measured at laboratory energies between 0.3 and 5.0 keV. Using reduced variables and an exponentially shielded Coulomb potential, we deduced, from the experimental differential cross sections, the crossing radius where the electron capture takes place. This analysis indicates that it occurs at a critical projectile-target separation between $1.63a_0$ and $2.21a_0$ in the energy range of the present study and that at least two different processes are involved. The participating states are not identified at this time.

The total cross section shows the presence of structures. These structures represent the participation of the ground electronic states and selected electronically excited states of the projectile and the target, which are in agreement with the results obtained from the differential cross sections.

ACKNOWLEDGMENTS

We are grateful to B. E. Fuentes for helpful suggestions and comments. We wish to thank A. González for his technical assistance. The research was supported by DGAPA under Grant No. IN-100392 and CONACYT under Grant No. 3659P-E9607.

[1] H. Martínez and J. M. Hernández, Chem. Phys. **215**, 285 (1997).
[2] H. Martínez, J. M. Hernández, P. G. Reyes, E. R. Marquina, and C. Cisneros, Nucl. Instrum. Methods Phys. Res. B **124**, 464 (1997).
[3] W. B. Maier II, J. Chem. Phys. **69**, 3077 (1978).
[4] H. Martínez, J. Phys. B **31**, 1553 (1998).
[5] F. T. Smith, R. P. Marchi, and K. G. Dedrick, Phys. Rev. **150**, 79 (1966).
[6] N. F. Mott and H. S. W. Massey, *The Theory of Atomic Collisions*, 3rd ed. (Oxford University Press, London, 1965), p. 662.
[7] W. B. Maier II, J. Chem. Phys. **60**, 3588 (1974).
[8] R. E. Olson, F. T. Smith, and E. Bauer, Appl. Opt. **10**, 1848 (1971).
[9] R. E. Olson, Phys. Rev. A **2**, 121 (1970).